Free–free absorption coefficients and Gaunt factors for dense hydrogen-like stellar plasma

V Srećković, N Sakan, D Šulić, D Jevremović, Lj Ignjatović, M Dimitrijević

Monthly Notices
of the
ROYAL ASTRONOMICAL SOCIETY
MNRAS **475,** 1131–1136 (2018) doi:10.1093/mnras/stx3237

Free–free absorption coefficients and Gaunt factors for dense hydrogen-like stellar plasma

V. A. Srećković,[1,2★] N. Sakan,[1★] D. Šulić,[3] D. Jevremović,[4] Lj. M. Ignjatović[1,2] and M. S. Dimitrijević[2,4,5★]

[1] *University of Belgrade, Institute of Physics, PO Box 57, 11001 Belgrade, Serbia*
[2] *Isaac Newton Institute of Chile, Yugoslavia Branch, Volgina 7, 11060 Belgrade, Serbia*
[3] *University Union – Nikola Tesla, 11000, Belgrade, Serbia*
[4] *Astronomical Observatory, Volgina 7, 11160 Belgrade 74, Serbia*
[5] *LERMA, Observatoire de Paris, PSL Research University, CNRS, Sorbonne Universités, UPMC (Univ. Pierre, and Marie Curie) Paris 06, 5 Place Jules Janssen, 92190 Meudon, France*

Accepted 2017 December 12. Received 2017 November 28; in original form 2017 October 25

ABSTRACT

In this work, we present a study dedicated to determination of the inverse bremsstrahlung absorption coefficients and the corresponding Gaunt factor of dense hydrogen-like stellar-atmosphere plasmas where electron density and temperature change in a wide range. A method suitable for this wide range is suggested and applied to the inner layers of the solar atmosphere, as well as the plasmas of partially ionized layers of some other stellar atmospheres (for example, some DA and DB white dwarfs) where the electron densities vary from 10^{14} cm^{-3} to 10^{20} cm^{-3} and temperatures from 6000 K to 300 000 K in the wavelength region of 10 nm $\leq \lambda \leq$ 3000 nm. The results of the calculations are illustrated by the corresponding figures and tables.

Key words: atomic processes – Sun: atmosphere – stars: atmospheres – white dwarfs.

1 INTRODUCTION

Although, of all the plasma internal absorption processes, we have so far considered only ion–atom radiative ones, we are aware of the need to consider other possible absorption processes too. Namely, some of them must be treated as concurrent to the ones that we have studied, and others warrant our attention for more diverse reasons. One such kind of process is that of electron–ion bremsstrahlung, which, by its very nature, suggests its importance, as its efficiency increases proportionally to the square of the free-electron density. Anyone interested in these processes must be fascinated by the amount of works about them. Indeed, so much has been done in this field that any new work should contain a very important result. However, we believe that for some time now we have had results of significant importance; we mean the possibility of determining the spectral characteristics of inverse bremsstrahlung (absorption coefficients and Gaunt factors) in the same way in a wide range of electron densities and temperatures. We note that some preliminary results have been presented at the X Serbian Conference on Spectral Line Shapes in Astrophysics (Mihajlov, Srećković & Sakan 2015), in order to inform other researchers of the potential possibilities existing in the field of inverse bremsstrahlung processes.

The aims of this work require determination of the corresponding spectral absorption coefficients for the inverse bremsstrahlung process and the corresponding Gaunt factors for a broad class of weakly non-ideal plasmas, as well as for plasmas of higher non-ideality. It is shown that this process can be successfully described in the frame of the cut-off Coulomb potential model within the range of the physical parameters that cover the area important for modelling astrophysical plasma (white dwarfs, solar atmospheres, etc). The physical sense and the properties of a group screening parameter for two-component systems that are used in this paper are discussed in detail in our previous papers (Mihajlov, Vitel & Ignjatović 2009a,b). This method for describing the electrostatic screening in two-component systems is applicable to systems of higher non-ideality degree. On the basis of data from the above-mentioned papers are determined new characteristic lengths that complete a new system of screening lengths in plasma. This topic itself, the discussion and search for more consistent models of screening and more realistic potentials in plasmas is still continuing and is very current (see Mihajlov et al. 2009b; Demura 2010, and references therein).

For the sake of further considerations, we will introduce some designations that are used below: E and E': respectively, the energies of the initial and final states of the electron–ion system (absorber); $\varepsilon_{\rm ph}$: the energy of the absorbed photon and $\hbar k$: its impulse; $\hbar q$: the impulse of the electron in its initial state; and m, e: respectively, the mass of the electron and the modulus of its charge.

★ E-mail: vlada@ipb.ac.rs (VAS); nsakan@ipb.ac.rs (NS); mdimitrijevic@aob.rs (MSD)

2 NECESSARY THEORETICAL REMARKS

2.1 The potential and electrostatic screening model

In Mihajlov et al. (2015) the significance of the model potential used in this paper was emphasized. One of the model Coulomb screening potentials, known as the cut-off potential, had already been introduced in Suchy (1964), and had been investigated in connection with the transport plasma properties in Mihajlov et al. (1986). This potential is given by

$$U(r) = \begin{cases} -\dfrac{e^2}{r} + \dfrac{e^2}{r_{\rm cut}} & 0 < r \le r_{\rm cut} \\ 0 & r_{\rm cut} < r, \end{cases} \quad (1)$$

where r is the distance from the coordinate origin and $r_{\rm cut}$ is a parameter defined and determined further on in the text.

This is the model, illustrated by Fig. 1, used in this work. Let us note that in Mihajlov et al. (2011) the universality of the screening model did not arise at all. However, in the case of the electron–ion inverse bremsstrahlung process, which is possible in plasmas with enormous differences in electron densities and temperature, the situation is the other way round. Namely, in this case we have to start from the inner plasma electrostatic screening model of any considered system and to solve the problem of its applicability. For that purpose we will first consider the models used in the papers that exist in the literature (Hazak et al. 2002; Armstrong et al. 2014; van Hoof et al. 2014).

One can see that the electron–ion scattering is treated in those models as scattering of the electron upon the adequate Debye potential. This fact is a serious handicap of the mentioned models, as was discussed in our previous papers.

This is caused by the fact that the Debye potential is defined as a potential of the observed ion and the entirety of its surrounding as a function of the distance from the ion, and can be used only for determination of its average potential energy in the observed plasma. Because of this, in Mihajlov et al. (2011) the model of the inner plasma screening was applied for the first time. Fig. 1 implies that in this screening model the potential energy of the free electron $U_{\rm scr.}(r)$ is of a strictly Coulomb nature: $U_{\rm scr.}(r) = -e^2/r$ in the region $r < r_{\rm cut}$, where $r_{\rm cut}$ is the corresponding cut-off radius, and $U_{\rm scr.}(r) = {\rm const} = U_{\rm cut}$ in the region $r > r_{\rm cut}$, where $U_{\rm cut}$ is equal to the average energy of the free electron in the considered system. In further consideration of this, we take $U_{\rm cut} = -e^2/r_{\rm cut}$ as the zero of the energy and describe such plasma just by means of the model cut-off potential given by equation (1), which is especially suitable for describing electron–ion scattering within plasma. Certainly, we assume that the above-described electrostatic screening model could be applicable in such a wide range of electron densities and temperatures that this allows one to consider it as an almost universal model. For that very reason the cut-off potential equation (1) could also be considered as almost universal.

2.2 Transformation of the dipole moments

It is only after an explanation of the universality of the potential equation 1 that the procedures gain importance for the determination of inverse bremsstrahlung processes as characteristic spectral absorption coefficients, Gaunt factors, and the possibility of improvement of these procedures.

As the first improvement, for the inverse bremsstrahlung cross-section $\sigma_{\rm i.b.}^{\rm (ex)}$, the standard expressions from Sobelman (1979) will be used here, since the potential equation (1) has a finite radius.

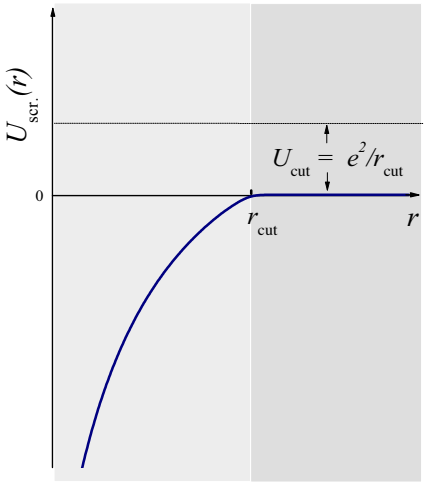

Figure 1. Behaviour of the potential $U_{\rm scr.}(r)$, where $r_{\rm cut}$ is the cut-off parameter presented in equations (6) and (7).

Consequently,

$$\sigma_{\rm i.b.}^{\rm (ex)}(E;E') = \frac{8\pi^4}{3}\frac{\hbar e^2 k}{q^2}\sum_{l'=l\pm1} l_{\rm max}|\hat{D}_{E,l;E'l'}|^2,$$

$$\hat{D}_{E,l;E'l'} = \int_0^\infty P_{E';l'}(r)\cdot r\cdot P_{E;l}(r){\rm d}r, \quad (2)$$

where $l_{\rm max}$ is defined in section 2.4, the radial functions $P_{E;\,l}(r)$ and $P_{E';l'}(r)$ are the solutions of the radial Schrödinger equation

$$\frac{{\rm d}^2 P_{E;l}(r)}{{\rm d}r^2} + \left[\frac{2m}{\hbar^2}(E - U(r)) - \frac{l(l+1)}{r^2}\right] P_{E;l}(r) = 0, \quad (3)$$

and $U(r)$ is the cut-off Coulomb potential given by equation (1). The radial functions $P_{E;\,l}(r)$ of all states that are possible in the potential $U(r)$ are described and discussed by Mihajlov et al. (1986). As the next step, using the transformation characteristics of the matrix element of the solutions $P_{E;\,l}(r)$ we will replace the dipole matrix element $\hat{D}_{E,l;E'l'}$ in equation 2 by the matrix element of the gradient of the potential energy $U(r)$. This procedure is described by the expressions

$$|\hat{D}(r)_{E,l;E'l'}|^2 = \frac{\hbar^4}{m^2\left(E - E'\right)^4}|\nabla U_{E,l;E'l'}|^2, \quad (4)$$

$$\nabla_r U_{E,l;E'l'} = \int_0^{r_{\rm cut}} P_{E,l}(r)\cdot\nabla_r U(r)\cdot P_{E'l'}(r){\rm d}r, \quad (5)$$

where $U(r)$ is given by equation (1).

It is known that the transition from the dipole matrix element $\hat{D}_{E,l;E'l'}$ to the dipole matrix element $\nabla_r U_{E,l;E'l'}$ in principle does not mean much. However, in the case of $U(r)$, which is given by equation (1), it means a transition from determination of the quantity $\hat{D}_{E,l;E'l'}$, which cannot be factually calculated, to determination of a quantity that can be calculated routinely. Namely, in the case of this potential the integral of two functions of the Coulomb continuum from 0 to ∞ gets replaced by the integral of the same two functions, but from 0 to $r_{\rm cut}$.

2.3 Determination of the cut-off radius

In order to complete the described model we have to determine the cut-off parameter $r_{\rm cut}$ and the energy parameter $U_{\rm cut}$ as functions of the electron density N_e and the temperature T. Here we will

Table 1. Values of the Gaunt factor for $N_e = 1 \times 10^{17}$ [cm^{-3}] as a function of wavelength λ and temperature T. The tables are available in their entirety for 10^{14} cm^{-3} to 10^{20} cm^{-3} and temperatures from 6000 K to 300 000 K in the wavelength region of 10 nm ≤ λ ≤ 3000 nm in machine-readable form in the online journal as additional data. A portion is shown here for guidance regarding their form and content.

λ [*nm*]/T [K]	10 000	20 000	40 000	50 000	100 000	150 000	200 000	250 000	300 000
10	1.084E+00	1.101E+00	1.121E+00	1.133E+00	1.207E+00	1.244E+00	1.291E+00	1.341E+00	1.415E+00
100	1.088E+00	1.104E+00	1.166E+00	1.217E+00	1.588E+00	1.813E+00	2.053E+00	2.303E+00	2.562E+00
200	1.093E+00	1.151E+00	1.402E+00	1.565E+00	2.522E+00	3.053E+00	3.609E+00	4.185E+00	4.778E+00
500	1.167E+00	1.512E+00	2.425E+00	2.932E+00	5.769E+00	7.322E+00	8.940E+00	1.061E+01	1.233E+01
1000	1.469E+00	2.340E+00	4.401E+00	5.533E+00	1.182E+01	1.524E+01	1.877E+01	2.240E+01	2.611E+01
1500	1.845E+00	3.251E+00	6.532E+00	8.330E+00	1.825E+01	2.359E+01	2.908E+01	3.469E+01	4.039E+01
2000	2.251E+00	4.207E+00	8.762E+00	1.125E+01	2.486E+01	3.213E+01	3.957E+01	4.715E+01	5.484E+01
2500	2.675E+00	5.197E+00	1.106E+01	1.424E+01	3.157E+01	4.075E+01	5.014E+01	5.968E+01	6.934E+01
3000	3.110E+00	6.216E+00	1.339E+01	1.729E+01	3.833E+01	4.942E+01	6.074E+01	7.223E+01	8.385E+01

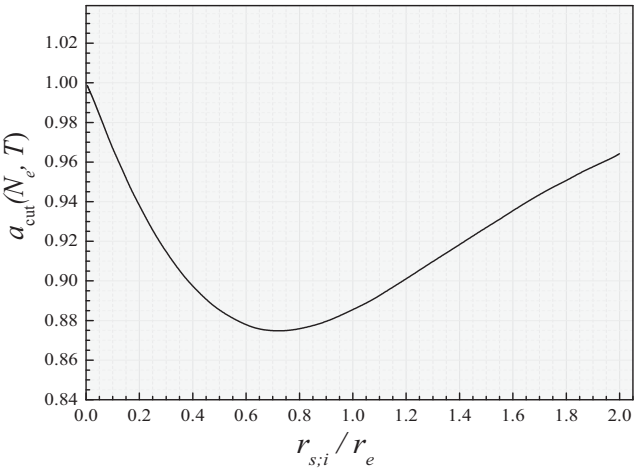

Figure 2. Behaviour of the parameters $a_{\rm cut} = r_{\rm cut}/r_e$ as a function of the ratio $r_{s;\,i}/r_e$, where r_e is given by equation (6) and $r_{s;\,i}$ is the ion Wigner–Seitz radius for the considered electron–ion plasma. The presented curve is obtained on the basis of data presented in Mihajlov et al. (2009a).

use the fact that these parameters can be determined by means of Fig. 2, which is obtained using the data from Mihajlov et al. (2009a). Namely, the curve presented in Fig. 2 shows the behaviour of the parameter $a_{\rm cut} = r_{\rm cut}/r_e$ as a function of the ratio $r_{s;\,i}/r_e$, where r_e and the ion Wigner–Seitz radius $r_{s;\,i}$ are given by the relations

$$r_{s;i} = \left[\frac{3}{4\pi N_i}\right]^{1/3}, \quad r_e = \left[\frac{kT}{4\pi N_e e^2}\right]^{1/2}, \tag{6}$$

where N_i is the ion density. After that the cut-off radius $r_{\rm cut}$ is determined here as a function of N_e, T by means of the relation

$$r_{\rm cut} = a_{\rm cut} \cdot r_e, \tag{7}$$

where the parameter $a_{\rm cut}$ can be directly determined from Fig. 2. The procedure for the determination of $a_{\rm cut}$ is to calculate the ratio $r_{s;\,i}/r_e$ (by equation 6) for the required values of plasma parameters (electron density and temperature) and to directly obtain (download) the y values on the curve in Fig. 2 for the known x value.

2.4 The numerical procedure

The numerical procedure consists of two important elements. The *first element* refers to the way of determining $P_{E;\,l}(r)$ in the area $r > r_{\rm cut}$. As known, the necessary solution of equation 3 is given by superposition of the spherical Bessel functions, i.e. $C_1 j_n(z) + C_2 y_n(z)$, where $j_n(z)$ and $y_n(z)$ are spherical Bessel functions of the first and second kinds and they are of the nth order. However, here is used the fact that these functions are expressed over the Coulomb functions $F_l(0, \frac{\sqrt{2mE}}{\hbar} r)$ and $G_l(0, \frac{\sqrt{2mE}}{\hbar} r)$ by means of the relations (see e.g. Gough 2009) $j_L(\rho) = \rho^{-1} F_L(0,\, \rho)$ and $y_L(\rho) = -\rho^{-1} G_L(0,\, \rho)$, where $G_L(0,\, \rho)$ is the Coulomb function that is irregular at the coordinate origin. In accordance with that, the necessary radial function $P_{E;\,l}(r)$ in the case $r > r_{\rm cut}$ is used here in the form

$$P_{E;l}(r) = C_N^c \left\{ C_F F_l \left(0, \frac{\sqrt{2mE}}{\hbar} r\right) + C_G G_l \left(0, \frac{\sqrt{2mE}}{\hbar} r\right) \right\}, \tag{8}$$

where C_N^c is the normalization constant and C_F and C_G are the constants that provide the behaviour of the solution according to the convergent value for infinite radii. In such a way, we have fully standardized the expressions for the necessary (continual) radial solutions of equation (3).

The *second element* of the numerical procedure refers to the method of summing in equation 2 for the inverse bremsstrahlung cross-section $\sigma_{\rm i.b.}^{\rm (ex)}(E; E')$. After a detailed investigation, the following method of summation is chosen: the sum goes over l' from 0 to $l_{\rm max}$ with no need for initial checking of the convergence, and for $l' > l_{\rm max}$ the sum is checked for convergence, e.g. when l' is greater than $l_{\rm max}$ the Cauchy criteria for the convergence test is applied since it is expected that the sum monotonically converges towards the limit value. The behaviour of the sum after reaching the limiting value $l_{\rm max}$ was examined and convergence is proved in the limiting series of $r_{\rm cut}$, when the cut-off radius converges towards infinity $r_{\rm cut} \to \infty$. To determine the start of the checking boundary we use $l_{\rm max} = \lfloor l^* \rfloor + 1$ where l^* is determined from the relation $\frac{\hbar^2 \cdot l(l+1)}{2mr_{\rm cut}^2} = E$ From here, keeping in mind that $l(l+1) = (l+1/2)^2 - 1/4$, we get the boundary value l^* in the form $l^* = 0.5 \cdot (\sqrt{1 + 8 \cdot \frac{2mE}{\hbar^2} r_{\rm cut}^2} - 1)$. It has been shown that summing over l in the region $l > l_{\rm max}$ ends very quickly, so that the total number of summands is not much greater than $l_{\rm max}$. Such behaviour of the sum is proof of a well defined $l_{\rm max}$ boundary. After these improvements we could use the possibilities provided by the universality of the electrostatic screening model that we used and finally perform extensive calculations of the inverse bremsstrahlung characteristics that could be the basis for creation of the corresponding data base.

3 THE CALCULATED QUANTITIES

We consider here plasmas with electron densities from 10^{14} cm^{-3} to $1 \cdot 10^{20}$ cm^{-3} and temperatures from 6000 K to 300 000 K. In

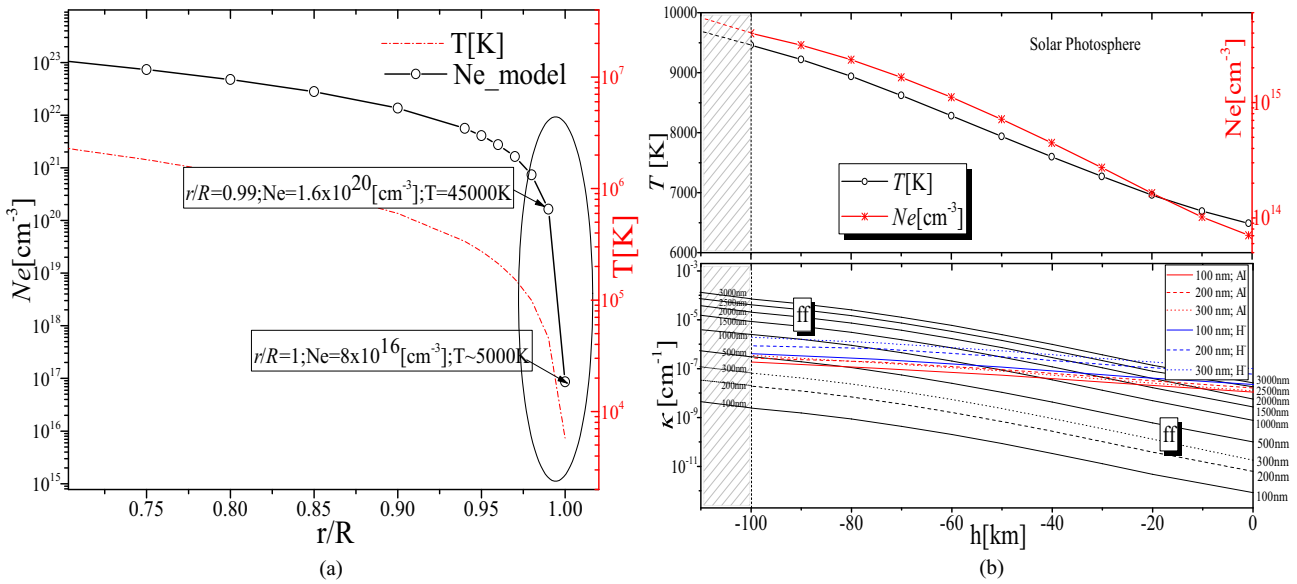

Figure 3. (a) Electron density and temperature in the interior of the Sun as a function of radius for the Standard Solar Models (Bahcall, Serenelli & Basu 2006). (b) Upper panel: behaviour of the temperature T and N_e as a function of height h within the considered part of the solar atmosphere model of Fontenla, Balasubramaniam & Harder (2007). Lower panel: plots of the absorption coefficients (equation (9)) of the absorption processes considered for the case of a solar atmosphere model from Fontenla et al. (2007). Black lines denote free–free (ff) absorption processes, i.e. inverse bremsstrahlung absorption coefficients, blue electron–atom and red ion–atom absorption coefficients (Ignjatović et al. 2014; Srećković et al. 2014). The extrapolated values are in the left shaded region in front of the dashed line.

accordance with Mihajlov et al. (1993) and Adamyan et al. (1994), for such conditions we find that, for the electron component, treated as an appropriate electron gas on a positively charged background, the value of the chemical potential is practically equal to the classical one, so that the distribution function for electrons is Maxwellian $f_T(v) = 4\pi(m/2\pi kT)^{3/2}v^2 e^{-mv^2/2kT}$, for a given temperature T. Consequently,

$$\kappa_{\text{i.b.}}^{(\text{ex})}(\varepsilon_\lambda; N_e, T) = N_e^2 \cdot \int_0^\infty \sigma_{\text{i.b.}}^{(\text{ex})}(E; E')v \cdot f_T(v)dv \cdot \left(1 - \exp\left[-\frac{\hbar\omega}{kT}\right]\right), \quad (9)$$

where the expression in parentheses takes into account the effect of stimulated emission. Additionally, we take the quasi-classical Kramer's $k_{\text{i.b.}}^{\text{q.c.}}(\lambda, T; Ne)$ (see e.g. Sobelman 1979) as

$$k_{\text{i.b.}}^{\text{q.c.}}(\lambda, T; Ne) = N_e^2 \cdot \frac{16\pi^{5/2}\sqrt{2}e^6}{3\sqrt{3}cm^{3/2}\varepsilon_{\text{ph}}^3} \frac{\hbar^2}{(kT)^{1/2}} \left(1 - \exp\left[-\frac{\hbar\omega}{kT}\right]\right), \quad (10)$$

where $\varepsilon_{\text{ph}} = 2\pi\hbar c/\lambda$, and the averaged Gaunt factor $G_{\text{i.b.}}(\lambda, T)$ is

$$k_{\text{i.b.}}^{(\text{ex})}(\lambda, T; N_e) = k_{\text{i.b.}}^{\text{q.c.}}(\lambda, T; N_e) \cdot G_{\text{i.b.}}(\lambda, T), \quad (11)$$

where $k_{\text{i.b.}}^{(\text{ex})}(\lambda, T; Ne)$ and $k_{\text{i.b.}}^{\text{q.c.}}(\lambda, T; Ne)$ are given by equations (9) and (10).

4 RESULTS AND DISCUSSION

The contribution of inverse bremsstrahlung to the total absorption in stellar atmospheres is not so important, but its contribution increases with density, and for very dense plasmas it becomes dominant. For example, Grinenko & Gericke (2009) stated that inverse bremsstrahlung is the dominant absorption mechanism for lasers with parameters typical for inertial confinement fusion. Plasma in inertial confinement fusion experiments has properties that are similar to the conditions in stellar interiors. Consequently, it is of interest to investigate the role of inverse bremsstrahlung in subphotospheric and deeper layers, and to examine its influence on radiative transfer through such layers.

In addition to other factors that determine the importance of inverse bremsstrahlung, we should bear in mind the existence of a physical area where inverse bremsstrahlung is dominant compared to other processes. The examples that demonstrate this can be found in the literature (Rozsnyai 2001; Grinenko & Gericke 2009). Moreover, we expect a major contribution to the inverse bremsstrahlung process in a dense highly ionized plasma (see e.g. Fig. 3(a), the marked region of r) in the process of transfer of radiation. Here we mean the high electron density and temperature that occur in the interior of the Sun, which are in Fig. 3(a) presented as a function of radius (Standard Solar Models, Bahcall et al. 2006).

In the lower panel in Fig. 3(b), the plot of each absorption coefficient of the considered absorption processes for the case of a solar atmosphere model from Fontenla et al. (2007) is shown as a function of height for various values of wavelengths. Here h is the height of the considered layer with respect to the chosen referent one. The corresponding plasma parameters are presented in the upper panel of Fig. 3(b). The electron–atom processes that are sometimes treated as the H^- continuum. With AI, i.e. κ_{ai}, atom–ion symmetric and non-symmetric processes (Ignjatović et al. 2014; Srećković et al. 2014) are represented. From this figure one can see that the inverse bremsstrahlung absorption coefficients are comparable with the concurrent ones, especially in the region of higher electron density and temperature $h \leq -70$ km (left-hand part of Fig. 3(b)). Consequently, we can conclude that the influence of the inverse bremsstrahlung process increases with temperature and density.

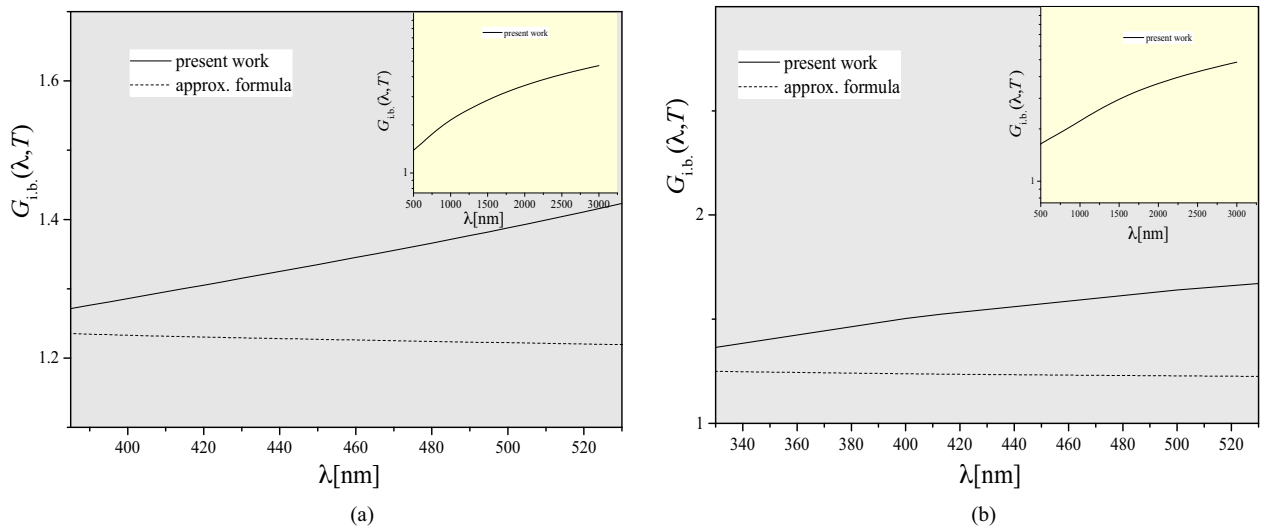

Figure 4. (a) Dynamics of the Gaunt factor data from this work (equation (11)) and data obtained by the approximation formula (D'yachkov 1990) for the electron density $N_e = 6.5 \cdot 10^{18}$ cm^{-3} and temperature $T = 18\,000$ K (from Vitel et al. 2004; Mihajlov et al. 2011). (b) Behaviour of the mean Gaunt factor data from this work and data obtained by the approximation formula (D'yachkov 1990) for the electron density $N_e = 1.5 \cdot 10^{19}$ cm^{-3} and $T = 23\,000$ K (from Vitel et al. 2004; Mihajlov et al. 2011).

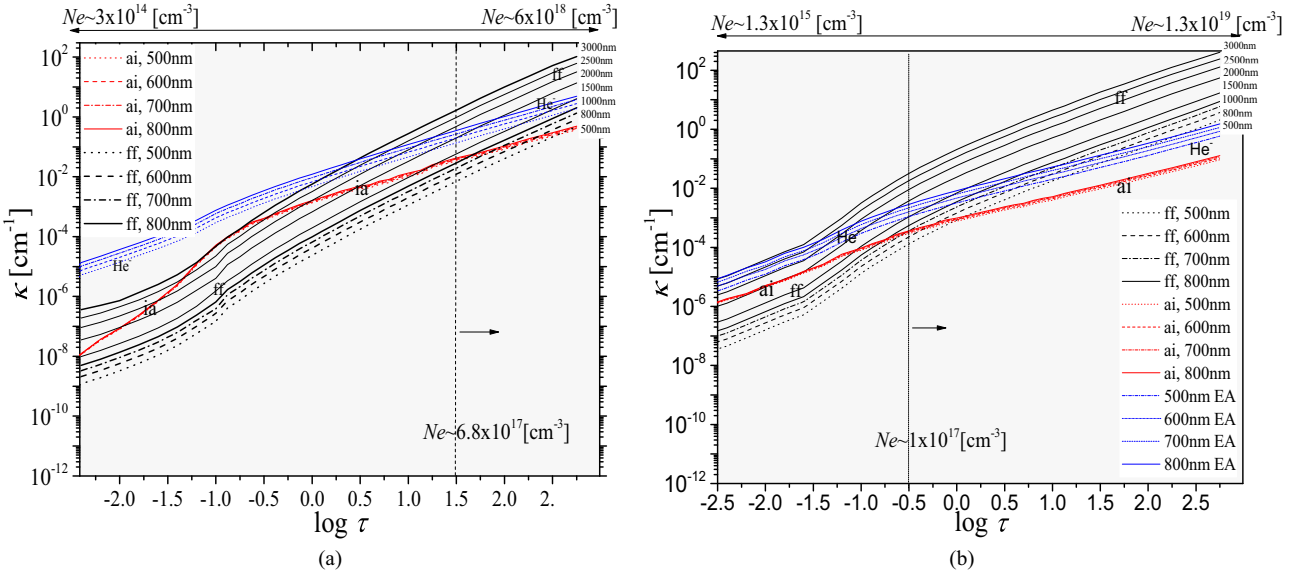

Figure 5. (a) Plots of the absorption coefficients (equation (9)) of the considered absorption processes for the case of a DB white dwarf with $T_{\rm eff} = 12\,000$ K and $\log g = 8$ as functions of $\log \tau$, where τ is the Rosseland optical depth. (b) Plots of the absorption coefficients (equation (9)) of the considered absorption processes for the case of a DB white dwarf with $T_{\rm eff} = 16\,000$ K and $\log g = 8$ as functions of $\log \tau$, where τ is the Rosseland optical depth. Black lines denote ff absorption processes, i.e. inverse bremsstrahlung absorption coefficients, blue concurrent electron–atom (EA) processes (He^- continuum) and red concurrent ion–atom absorption coefficients (ai).

The behaviour of the Gaunt factor in the area of higher parameters of non-ideality is shown in Figs 4(a) and (b). In these figures are presented the dynamics of the Gaunt factor for the electron density $N_e = 6.5 \cdot 10^{18}$ cm^{-3} and temperature $T = 18\,000$ K as well as for $N_e = 1.5 \cdot 10^{19}$ cm^{-3} and $T = 23\,000$ K (parameters obtained in the experiment by Vitel et al. 2004; Mihajlov et al. 2011). The data from this work are marked by solid lines and data obtained by the use of the approximation formula (D'yachkov 1990) by the dashed line. The insets show the data from this work but in a wider wavelength region. One can notice that there is an evident difference between the data presented here and data obtained by the use of the approximation formula (D'yachkov 1990). These differences are affected by the principal differences in the way of describing the electron–ion scattering in the rest of the plasma (see Mihajlov et al. 2009a). It is understood that some of these results may be useful for further laboratory plasma investigations.

Good conditions for studying the impact of the increase of electron density and temperature on the inverse bremsstrahlung contribution is provided by plasmas of white dwarf atmospheres. This is illustrated in Figs 5(a) and (b), where the plots of the considered absorption processes, including the inverse bremsstrahlung processes, are shown for the case of a DB white dwarf with $\log g = 8$, $T_{\rm eff} = 12\,000$ K and $T_{\rm eff} = 16\,000$ K from the atmosphere model

of Koester (2015, private communication). The electron–atom processes (He^- continuum), are represented in these figures by blue lines marked by EA (κ_{EA}). ai, i.e. κ_{ai}, represents atom–ion symmetric and non-symmetric processes. From these figures one can see that the inverse bremsstrahlung absorption coefficients are comparable with concurrent ones, especially in the region of higher electron density (the parts of Figs 5(a) and (b) marked with arrows). Finally, within the considered DB white dwarf atmospheres, the investigated radiative processes strongly influence the atmosphere's opacity, especially for the cases of white dwarf atmospheres with larger effective temperature, i.e. higher electron densities and temperatures.

Concerning the accuracy, a number of factors may affect it. First, we discuss the screening parameters. It is likely that such a change in the screening length will affect the accuracy. Since the method that is used here is applicable to systems of higher non-ideality degree, its use is limited to certain areas of plasma temperatures and densities. For plasmas with low non-ideality (i.e. low density and high temperature) or plasmas with extreme non-ideality with the coupling parameter Γ much greater than 1 (high density and very low temperature), this approach is not capable of providing high accuracy (here $\Gamma = e^2/(akT)$ and $a = (3/4\pi N_e)^{1/3}$). Finally, we are also able to notice that the data are highly sensitive to changes in temperature.

To summarize, the presented exact quantum-mechanical method is used to obtain the spectral coefficients for the inverse bremsstrahlung process and the corresponding Gaunt factors for a broad class of moderately non-ideal plasmas, as well as for plasmas of higher non-ideality. The range of the physical parameters covers the area important for plasma modelling from an astrophysical standpoint (white dwarfs, central stars of planetary nebulae, etc). For this purpose, calculation of the Gaunt factors in a wide region of wavelengths for series of electron densities and plasma temperatures was done. The results of the calculations are illustrated by the corresponding tables in the online version of this article (table for every N_e and T taken).

Further directions in the development of the method would be determination of absorption coefficients and Gaunt factors for two-component systems (ions with an arbitrary charge Z and electron component) as well as for three-component systems.

ACKNOWLEDGEMENTS

We acknowledge the contribution of the late Dr A. A. Mihajlov, who participated in the discussions and preparation of this paper. This work is partially supported by the Ministry of Education, Science and Technological Development of the Republic of Serbia under grants III 44002 and 176002.

REFERENCES

Adamyan V. M., Djuric Z., Ermolaev A. M., Mihajlov A. A., Tkachenko I. M., 1994, J. Phys. D, 27, 927
Armstrong G. S. J., Colgan J., Kilcrease D. P., Magee N. H., 2014, High Energy Density Phys., 10, 61
Bahcall J. N., Serenelli A. M., Basu S., 2006, ApJS, 165, 400
D'yachkov L. G., 1990, J. Phys. B, 23, L429
Demura A. V., 2010, Int. J. Spectrosc., 2010, 671073
Fontenla J. M., Balasubramaniam K. S., Harder J., 2007, ApJ, 667, 1243
Gough C., 2009, GNU Scientific Library Reference Manual—Third Edition. Network Theory Ltd., available online at: http://www.gnu.org/software/gsl/
Grinenko A., Gericke D. O., 2009, Dense plasma heating by inverse Bremsstrahlung, in: Central Laser Facility, Annual Report 2008/2009, Science and Technology Facilities Council, Rutherford Appleton Laboratory, Harwell Science and Innovation Campus, Didcot, Oxfordshire, p. 110
Hazak G., Metzler N., Klapisch M., Gardner J., 2002, Phys. Plasmas 9, 345
Ignjatović L. M., Mihajlov A. A., Srećković V. A., Dimitrijević M. S., 2014, MNRAS, 441, 1504
Mihajlov A. A., Djordjević D., Vučić S., Kraeft W. D., Luft M., 1986, Contr. Plasma Phys., 26, 19
Mihajlov A. A., Ermolaev A. M., Djurić Z., Ignjatović L., 1993, J. Phys. D, 26, 1041
Mihajlov A. A., Vitel Y., Ignjatović L. M., 2009a, High Temperature, 47, 1
Mihajlov A. A., Vitel Y., Ignjatović L. M., 2009b, High Temperature, 47, 147
Mihajlov A. A., Sakan N. M., Srećković V. A., Vitel Y., 2011, J. Phys. A, 44, 095502
Mihajlov A. A., Srećković V. A., Sakan N. M., 2015, JA&A, 36, 635
Rozsnyai B. F., 2001, J. Quant. Spectrosc. Radiative Transfer, 71, 655
Sobelman I. I., 1979, Atomic Spectra and Radiative Transitions. Springer, Berlin
Srećković V. A., Mihajlov A. A., Ignjatović L. M., Dimitrijević M. S., 2014, Advances Space Res., 54, 1264
Suchy K., 1964, Beitr. Plasmaphys. 4, 71
van Hoof P. A. M., Williams R. J. R., Volk K., Chatzikos M., Ferland G. J., Lykins M., Porter R. L., Wang Y., 2014, MNRAS, 444, 420
Vitel Y., Gavrilova T. V., D'yachkov L. G., Kurilenkov Y., 2004, J. Quant. Spectrosc. Radiative Transfer, 83, 387

SUPPORTING INFORMATION

Supplementary data are available at *MNRAS* online.

Additional Supporting Information (tables) may be found in the online version of this article. The tables are available in their entirety for 10^{14} cm^{-3} to 10^{20} cm^{-3} and temperatures from 6000 K to 300 000 K in the wavelength region of 10 nm $\leq \lambda \leq$ 3000 nm in machine-readable form in the online journal as additional data.

Table 1. This table gives values of the Gaunt factor for $N_e = 1 \times 10^{17}$ [cm^{-3}] for temperatures 10 000 K $\leq T \leq$ 300 000 K in the wavelength region 10 nm $\leq \lambda \leq$ 3000 nm.

Please note: Oxford University Press is not responsible for the content or functionality of any supporting materials supplied by the authors. Any queries (other than missing material) should be directed to the corresponding author for the article.

This paper has been typeset from a TEX/LATEX file prepared by the author.